Supplementary material

$|\Psi\rangle_{\mathbf{RVB}}$ HAS NO AA (BB) PAIRING

In the main text, we have illustrated why the leading order contribution of NNN pairing vanishes in $|\Psi\rangle_{\rm RVB}$. Here we would like to show that, indeed, all the AA (BB) pairing vanish in $|\Psi\rangle_{\rm RVB}$ exactly up to any order in c. As explained in the text, the pairing amplitude between two sites i and j is given by the sum of all teleportation paths that connect i and j. As seen in Fig. 1, the solid red line a is a typical teleportation path that contributes to the pairing (ij). According to the local rule of the teleportation path (each path must turn at a vertex), it is not hard to see that any teleportation path contributing to the AA (BB) pairing must go through an odd number of corners and an even number of links. On the other hand, for a given teleportation path a, we can always find a dual teleportation path b which goes though the same number of corners and links. For any pair of dual a and b paths, the sign contribution from all the links (corners) are the same (opposite). Therefore, the total contribution from the pair of teleportation paths a and b always vanishes. Thus, we have proved that $|\Psi\rangle_{\rm RVB}$ has no AA (BB) pairing.

STRING PICTURE

Since the RVB bonds only connect sites on different sublattices, we can view such a RVB state as a liquid state of oriented strings. Indeed, choosing a reference VB_0 configuration, any VB configuration can be viewed as a closed oriented string configuration: the RVB bonds in the VB configuration are regarded as a piece of the closed string pointing from the A to the B sublattice, while the RVB bonds in the reference VB_0 configuration are regarded as the complementary piece pointing from the B to the A sublattice.

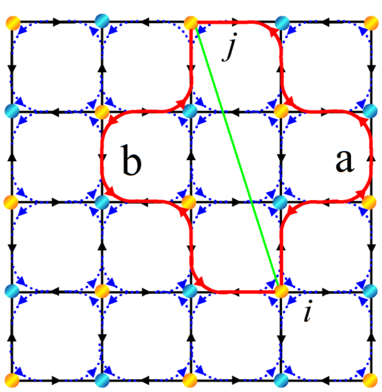

FIG. 1: (Color online) For any teleportation path contributing to the AA (BB) pairing, there always exists a dual teleportation path with opposite sign. Therefore the AA (BB) pairing amplitudes are exactly zero in $|\Psi\rangle_{\rm RVB}$.

If such a superposition of closed orientable string states indeed represent a *liquid* state of closed strings, then the entanglement entropy for a such a state in a region A has the form $S_A = aL_A - \frac{1}{2}\ln L_A + b$, where L_A is the length of the perimeter of region A. To understand such a result, we view a string as a flux line and the close-string condition implies that the flux is conserved. Therefore, the total flux going through the perimeter of A is zero. If we had ignored the flux conservation and assumed that the flux could fluctuate freely and independently, then the entanglement entropy would have an exact area-law form $S_A = aL_A$ and the typical amount of flux through the perimeter would be proportional to $\sqrt{L_A}$. So if we restrict the amount of flux through the perimeter to be zero, the entanglement entropy will be $S_A = aL_A - \ln\sqrt{L_A} + b = aL_A - \frac{1}{2}\ln L_A + b$. The $\ln L_A$ dependence in the entanglement entropy implies that the liquid of orientable closed strings must be gapless. This property is confirmed by our numerical calculation.

FINITE SIZE EXTRAPOLATION OF THE OPTIMUM PARAMETER c

We provide here a more accurate determination of the optimum parameter c. For this purpose, we use a quadratic function to fit the even sector ($|\Psi\rangle_e$) energy of a finite width (N_v) strip as a function of parameter c (around the minimum), and we extract the optimum parameter $c_{\rm opt}(N_v)$ and the minimum energy $E_{\rm min}(N_v)$ for $N_v = 10, \cdots, 24$. The results are presented in Fig. 2(a). Taking the optimum parameter $c_{\rm opt}(N_v)$ and extrapolating it to the thermodynamic limit as a function of inverse width $1/N_v$, we find $c_{\rm opt}(\infty) = 0.356(1)$ (see Fig. 2(b)). Again, taking the minimum finite width energy $E_{\rm min}(N_v)$ and extrapolating it to the thermodynamic limit as a function of $1/N_v$, we obtain a thermodynamic energy $E_\infty = -0.48620(1)$ (see Fig. 2(c)).

ENTANGLEMENT SPECTRA AND BOUNDARY HAMILTONIAN

Entanglement spectra (ES) and boundary Hamiltonian reflect rich information about the bulk of the system. Previous study has found that a gaped bulk phase with local order corresponds to a boundary Hamiltonian with local interactions, whereas critical behavior in the bulk is reflected on a diverging interaction length of the boundary Hamiltonian [1]. Here we study both ES and bound-

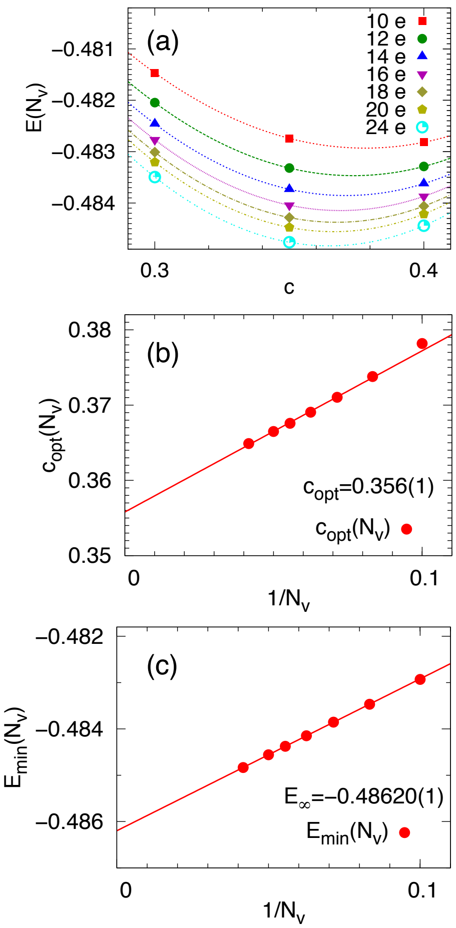

FIG. 2: (Color online)(a) A quadratic fit of the even sector energy $E(N_v)$ of a strip as a function of c around its minimum with $N_v = 10, \cdots, 24$. (b) Optimum parameter $c_{\rm opt}(N_v)$ plotted as a function of $1/N_v$. A linear regression gives $c_{\rm opt}(\infty) = 0.356(1)$. (c) Minimum energy $E_{\rm min}(N_v)$ plotted as a function of $1/N_v$. A linear regression gives $E(\infty) = -0.48620(1)$.

ary Hamiltonian by partition an infinite cylinder into two semi-infinite cylinders.

One of the virtue of PEPS description is that there is a duality mapping between the bulk and its boundary. This exact mapping is explained in detail in Ref. [1, 2], we only outline the key relations in defining ES and boundary Hamiltonian.

The boundary Hamiltonian H_b is defined from the reduced density operator (acting on the edge degrees of freedom) as $\sigma_b^2 = \exp(-H_b)$, and $\sigma_b^2 = \sigma_{bL}^2 = \sigma_{bR}^2$, here σ_{bL}^2 (σ_{bR}^2) is the reduced density operator of the left (right) half cylinder taking the form of $\sigma_{bL}^2 = \sqrt{\sigma_L^t}\sigma_R\sqrt{\sigma_L^t}$ ($\sigma_{bR}^2 = \sqrt{\sigma_R^t}\sigma_L\sqrt{\sigma_R^t}$). Here $\sigma_{L/R}$ are obtained by contracting the tensors of the left (right) half cylinders column-wise from the cylinder boundary to its edge. Note that to obtain $\sigma_{L/R}$ for an infinite cylinder, one starts from an initial vector and continuously applies the transfer matrix to the vector until it converges. The

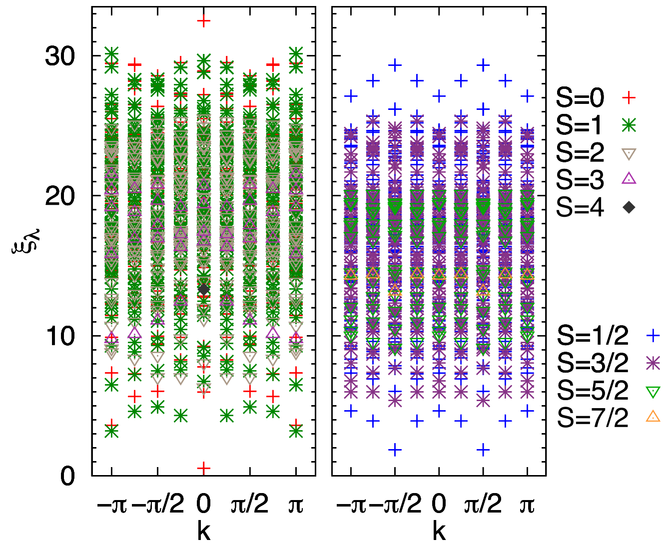

FIG. 3: (Color online) Entanglement spectra of a $N_v = 8$ cylinder as a function of momentum k winding around the cylinder and its total spin S for even and odd sectors without vison line in the wavefunction. The normalization for both sector are $\mathrm{Tr}\{\sigma_{L,p}^t\sigma_{R,p}\} = 1$, $p = e, o$. Plot is at the best variational parameter $c = 0.35$.

reduced density matrix of the left (right) half cylinder is $\rho_{L/R} = U\sigma_{bL/R}^2 U^\dagger$, where U is an isometry that maps any operator defined on the bulk onto the virtual spins [1]. By definition $\rho_{L/R}$ and $\sigma_{bL/R}^2$ share the same spectra.

Since the transfer matrix conserves the even or odd parity quantum number, one can define a mixed reduced density operator by writing $\sigma_{L/R} = \sigma_{L/R,e} + \sigma_{L/R,o}$ and $\sigma_{bL}^2 = \sqrt{\sigma_{L,e}^t}\sigma_{R,e}\sqrt{\sigma_{L,e}^t} + \sqrt{\sigma_{L,o}^t}\sigma_{R,o}\sqrt{\sigma_{L,o}^t}$, (similar definition applies to σ_{bR}^2), here the equal weight normalization condition is $\mathrm{Tr}\{\sigma_{L,e}^t\sigma_{R,e}\} = \mathrm{Tr}\{\sigma_{L,o}^t\sigma_{R,o}\} = 1$. The boundary Hamiltonian is thus uniquely defined, which we denote as $H_{\rm local}$. The reduced density operator $\sigma_{bL/R,p}^2$ in each sector $p = e, o$ contains a finite fraction of zero-weight eigenvalues.

We present the ES $\{\xi_\lambda\}$ of the boundary Hamiltonian $H_{\rm local}$ ($\sigma_b^2 = V\exp(-\mathrm{diag}\{\xi_\lambda\})V^\dagger$) as a function of momentum k around the cylinder and its total spin S in Fig. 3. The spin multiplet structure is inherited from the spin $1/2 \oplus 0$ representation of su(2) symmetry of the boundary Hamiltonian. One of the signatures of the ES is that the lowest excitation energy $\Delta(S) = \xi(S)_{\rm exc} - \xi_0$ does not vanish at infinite cylinder when scales linearly as a function of inverse cylinder parameter N_v, as depicted in Fig. 4(a), which however is in sharp contrast to the the case of Kagome nearest neighbor RVB state [2] that has been proved to be a gaped $\mathbb{Z}_2$ topological state [3].

To further explore the boundary theory, we expand the boundary Hamiltonian into 3^{2N_v} orthogonal operators, each of them is a product of any 9 local normalized orthogonal operators $\{\hat{x}_0, \cdots, \hat{x}_8\}$ defined as in Ref. [2].

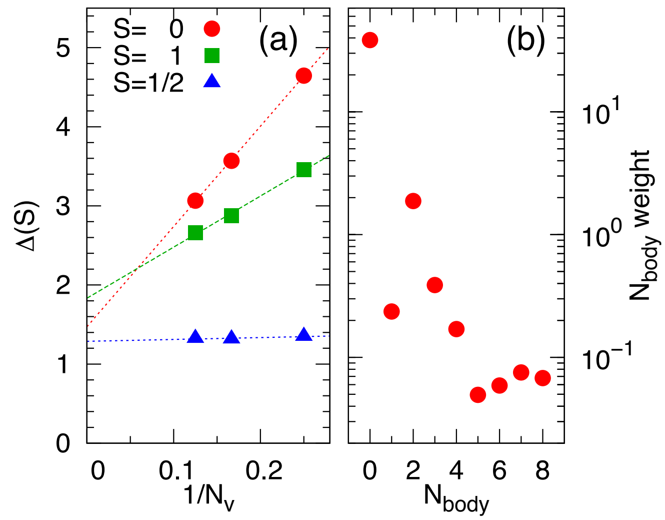

FIG. 4: (Color online) (a) The lowest energy gap $\Delta(S) = \xi(S) - \xi_0$ as a function of inverse cylinder parameter N_v. Fitted lines are of the form $\Delta(S) = \Delta(S)_{\rm inf} + a_S/N_v$; the excitation gap at infinite cylinder limit $\Delta(S)_{\rm inf}$ are finite for total spin $S = 0, 1/2, 1$. (b) N-body weight of the boundary Hamiltonian expanded in local operators $\{\hat{x}_0, \cdots, \hat{x}_8\}$ for a $N_v = 8$ cylinder. Both plot are at the best variational parameter $c = 0.35$.

The weight of N-body terms for a $N_v = 8$ cylinder is calculated and plotted in Fig. 4(b). The boundary Hamiltonian is clearly neither local nor short ranged, which is reflected from a flat fat tail for N-body ($N > 4$) terms in Fig. 4(b). This serves as a side evidence that the bulk is not gaped.

[1] J. I. Cirac, D. Poilblanc, N. Schuch and F. Verstraete, Entanglement spectrum and boundary theories with projected entangled-pair states, Phys. Rev. B **83**, 245134 (2011).

[2] D. Poilblanc, N. Schuch, D. Perez-Garcia and J. I. Cirac, Topological and entanglement properties of resonating valence bond wave functions, Phys. Rev. B **86**, 014404 (2012).

[3] N. Schuch, D. Poilblanc, J. I. Cirac and D. Perez-Garcia, Resonating valence bond states in the PEPS formalism, Phys. Rev. B **86**, 115108 (2012).